Structural Changes In Cytofluorescence Information Entropies With Histogram's Ranges Reduction For Medical Diagnostics

Nikolay E.Galich
Department of Experimental Physics, St. Petersburg State Polytechnical University
E-mail: n.galich@mail.ru

Abstract

New nonlinear methods of fluorescencel analysis of peripheral blood neutrophils have been developed. We used a sensitive technology of respiratory burst reaction of DNA fluorescence in the cells nuclei due to oxidative activity. Histograms in flow cytometry experiments are considered. Fluorescence flashes frequency as functions of fluorescence intensity are analyzed. Information entropies for standard deviation of immunofluorescence distributions and Hurst exponents are analyzed for histogram's ranges. Statistic peculiarities of histograms set for healthy and unhealthy donors allow dividing all histograms on the three classes for healthy donors and donors with oncology/autoimmune and inflammatory diseases. Alterations of immunofluorescence-net statistics and fractal dimensions in diagnostics of different diseases in various medical treatments have been demonstrated and discussed.

1 Introduction

Novel nonlinear statistical methods of immunofluorescence analysis are presented. Experimental data of DNA fluorescence in neutrophils nuclei of peripheral blood are investigated. Histograms of fluorescence are generated by flow cytometry method. Histograms describe fluorescence flashes frequency as functions of fluorescence intensity. Large-scale averaging of Shannon information entropy for initial histograms gives quality different of immunofluorescence statistical distributions for healthy and unhealthy donors.

Histograms of fluorescence contain a lot of information. Sense and value of the largest part of this information are unknown and only yet must be extracted. We examined one of possible approaches in this direction, connected with the nonlinear statistical analysis of immunofluorescence data for DNA of neutrophils. Neutrophils present one of the most important consistencies elements of immune system. Usage the technology of respiratory burst reaction of DNA fluorescence in neutrophils nuclei visualizes collective pictures of all pathological processes for oxidative activity of DNA [1-5].

Non-Gaussian fast exponential growth of central moments for fluorescence intensity fluctuations causes strong difficulties for strict, precise, quantitative interpretations of experimental results [5].Three illustrations are shown in Figs.1 [5]. Average value of intensity is smallest than dispersion, asymmetry and others higher statistical moments of intensity fluctuations, as it is shown in Fig.1b. Therefore standard statistical methods failed.

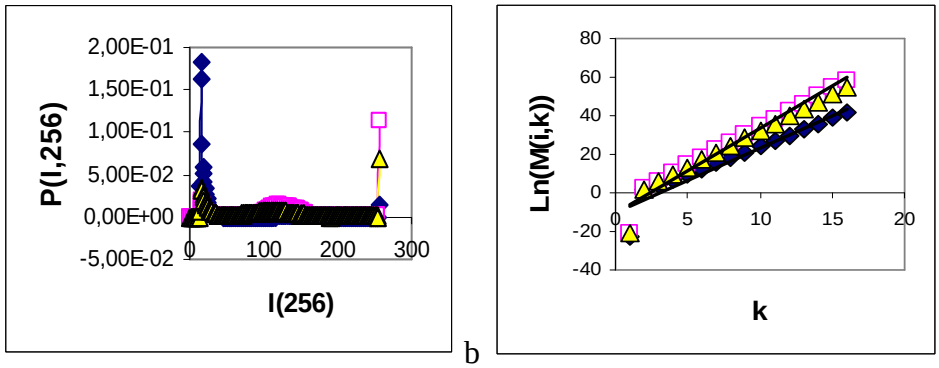

a b

Figs.1 (a) Dependence of spontaneous fluorescence flashes number $P(I,256)$ on their

intensity $I(256)$, non-dimensional variables; area under the final histograms normalized to unit; rhomb points correspond to bronchial asthma; quadrate points correspond to healthy donor; triangle points correspond to oncology disease. Common number of channels for fluorescence intensity $I(256)$ measurements is 256 (b) Logarithmic distributions of intensity central moments $Ln(M(i,k))$ as function on their number k for histograms in Fig.1a. Details are described in [5].

Previous analysis [4, 5] gives the classification for all sets of immunofluorescence histograms. This classification divides all donors on three big groups of health statuses. Fist group corresponds to healthy people. Second group corresponds to autoimmune and oncology diseases. Third group corresponds to inflammation diseases. We move further in the direction of understandings of the immunofluorescence nets structure for medical diagnostics.

2 Methods

Experimental methods and procedures were described in [4, 5]. Experiments based on the flow cytometrical measurement of the capability of the peripheral blood neutrophils for reaction of respiratory burst or oxidizing explosion [1-5]. We used hydroethidine addition with concentration 150 μg/ml for fluorescence initiation. Details of experimental procedures are described in [3,5]. The fragments of nuclear and mitochondrial DNA with oxidizing metabolism activity and oxidants [2, 3, 5] determine the basic place for localization of the fluorescent dye [1-3, 5], its distribution and concentration, and consequently intensity and statistics of fluorescence. Data analysis methods are interconnected with histograms simplification of Shannon information entropy distributions and calculations of corresponding Hurst exponents.

Sequences of large-scale averaging for histograms of Shannon information entropy distributions are analyzed. Square of relative deviations of fluorescence flashes number from their average level [5] determines the probability measure of immunofluorescence distributions for Shannon entropy. We use the centered random variables and their centered moments for all procedures on any step. This approach is necessarily for exception of the uncontrollable and systematic errors, instabilities of algorithmic procedures and corresponding drift of averages. Let us consider the relative deflections of fluorescence flashes number from their average level

$$n = (P_l - < P >) = < P > \times (\frac{N}{< N >} - 1), \qquad (1)$$

$< P >= (I_{\max} - I_{\min})^{-1}$, $N = N(l)$, $< N >= N_0 \times < P >$, $P_l = N(l)/N_0$, $l = 1,2,...256$,

where symbol $< ... >$ denotes statistical average of the fluorescence fluctuations for all 256 channels of intensity measurement ; $P_l = N(l)/N_0$ is the probability distribution density of the flashes number ; $N = N(l)$ is the number of flashes with the assigned intensity $I = l$ for the dimensionless intensity I coincides with the number of channels l ; N_0 is common number of flashes; average value of flashes number is $< N >= N_0 \times < P >$. Mean probability value is $< P >= (I_{\max} - I_{\min})^{-1} = 0.03906$ for 256 channels of intensity measurement.

Let us consider a square of the relative deviations of flashes numbers from the average level as the probability measure of the immunofluorescence fluctuations. Then probability of the immunofluorescence fluctuations for square of deviations is

$$p_l(n) = (n_l)^2 / \nu_n \ , \ \nu_n = \sum_{l=1}^{l=256} (n_l)^2 \qquad (2)$$

Let us introduce Shannon information entropy

$$E = -\sum_{l=1}^{l=256} p_l \times Ln(p_l) \qquad (3)$$

Probability density distribution of Shannon information entropy is

$$e(l) = -p_l \times Ln(p_l)/E \qquad (4)$$

Histogram's ranges reduction are similar to the sequential conversions of initial measurements of intensity I with 256 channels to a smaller number of channels and the final reduction to four channels of measurements. In this case the histogram's range is determined as maximal numbers of channels for every step of histogram averaging. Were analyzed the artificially increased sizes of observed measurement clusters on the structural features of fluorescence correlations, which vary in the dependence of averaging scale i.e. scale of intensity. Structure of histograms for entropy distributions, of somewhere between 256 and 4 on the scale of fluorescence intensity measurements, can be surprisingly complex, especially for autoimmune and oncology diseases. First and final steps of these procedures are shown in Figs.2.

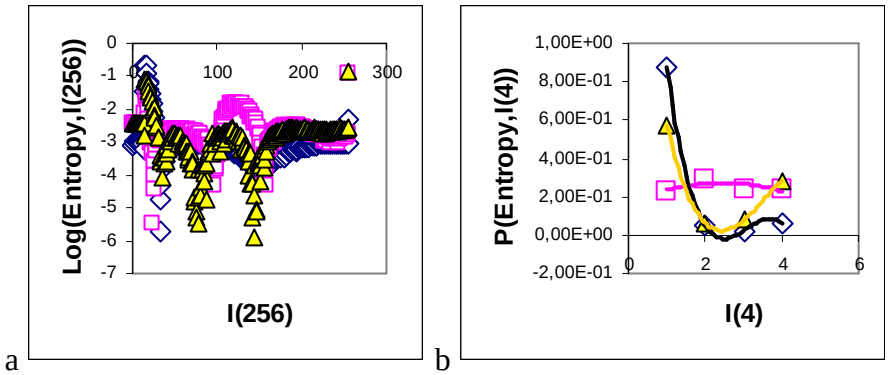

a b

Figs.2(a) Logarithm of Shannon information entropy e(I(256))as function on their intensity I(256) for histograms in Fig.1a; (b) Dependence of information entropy e(I(4)) on their intensity I(4) for histograms in Fig.2a; number of channels for the averaged fluorescence intensity I is 4, I(4)

More simple results are observed for minimal histogram's range in Fig.2b. In Fig.2b the good health man condition (square points) describes by means of convex parabola for parabolic approximation of entropy distribution e(I(4)). In Fig.2b the oncology describes by means of concave parabola for parabolic approximations of information entropy distributions e(I(4)). In Fig.2b the bronchial asthma describes by means of concave-convex parabola for parabolic approximations of information entropy distributions e(I(4)). So we have only three types of averaged long-scale e(I(4)) distributions, instead of very complex initial multi-channel entropy histograms e(I(254)).

Let us consider, briefly, fractal features of immunofluorescence (oxidative activity) nets, comparing the results of investigating the three initial immunofluorescence histograms for different donors in Fig. 1a. Results are shown in Figs. 3.

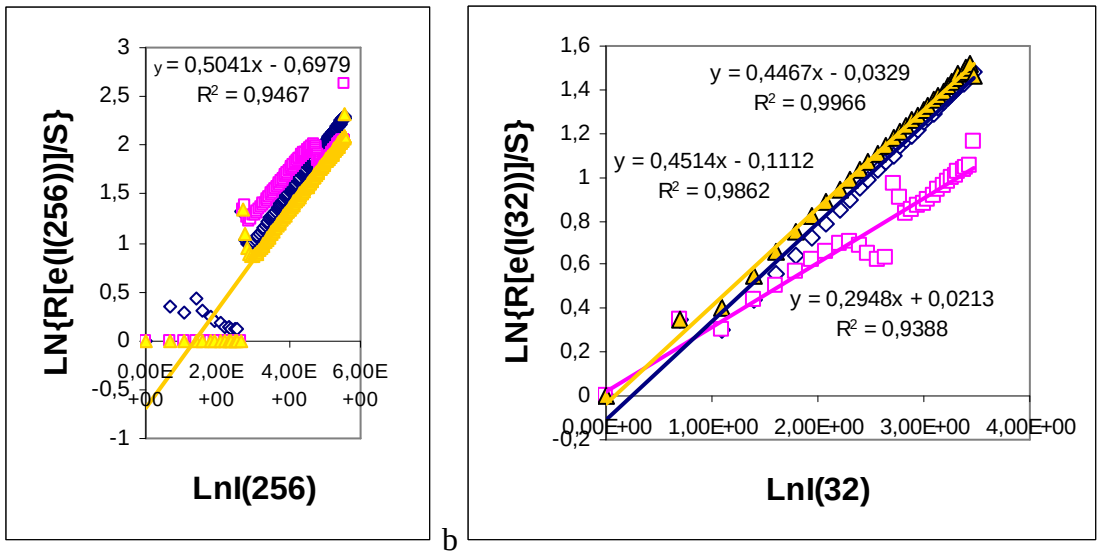

a b

Figs.3 (a) Hurst exponents $H_H(R(e(I(256)))/S)$, $H_H = \partial Ln(R/S)/\partial LnI$; rhomb points correspond to bronchial asthma, quadrate points correspond to the healthy donor, and triangle points correspond to the oncology disease. Initial histograms are shown in Fig.1a. (b) Hurst exponents $H_H(R(e(I(32)))/S)$ for initial histograms in Fig.2a; number of channels for the averaged fluorescence intensity I is 32, I(32)

Hurst exponent H_H [6] is determined by means of regression equation

$$Ln(R/S) = H_H \times LnI + const \qquad (5)$$

where R/S is rescaled range ($R = S$), R is range or maximal deviation of $e(I)$ from local mean level, S is standard deviation of $e(I)$. Hurst index H_H of Shannon entropy distribution $e(I)$ corresponds to its fractal (Hausdorff) dimension D_H [6] if

$$D_H = 2 - H_H \qquad (6)$$

In particular, the H_H exponent indicates persistent or correlated (H_H > ½) and anti-persistent or uncorrelated (H_1 < ½) behavior of the trend. Persistent behaviors are observed in Fig.3a with $H_H(R(e(I(256)))/S) = 0{,}5028$ for asthma, $H_H(R(e(I(256))/S) = 0{,}4202$ for healthy human and $H_H(R(e(I(256))/S) = 0{,}504$ for oncology. Correspondence fractal dimensions for histogram's range 256 are $1 < D_H < 1{,}6$.

Histogram's ranges reduction gives quality different Hurst exponents for different three groups of diseases, as it is shown in Fig.3b. Stratification of Hurst exponents in Fig.3b in the contrast from of Fig.3a testifies about structural changes of connections in immunofluorescence networks with measurements scale increasing or range reduction. Moreover, Hurst exponents can to change the sign for I-range=16, 8, 4 (see Fig.4). Some of these experimental observations (H <0) is contrary to standard textbook descriptions of Hurst index. Exactly the same discrepancy occurs with the experimental observations in geophysics [8, 9], financial markets [7] and other practical information.

Dynamics of Hurst exponent changes due to histogram's ranges reduction can not serve as very clear criterion for estimation of health statuses. Good health corresponds to anti-persistent behavior of H<0,5, for range number less than 200. Unhealthy people corresponds to persistent behavior of H>0,5, for range number more than 64. From this point of view the noticeable dominant of anti-persistent immune reaction for healthy people gives richer spectra of immunity surprises. Corresponding illustrations are shown in Fig.4.

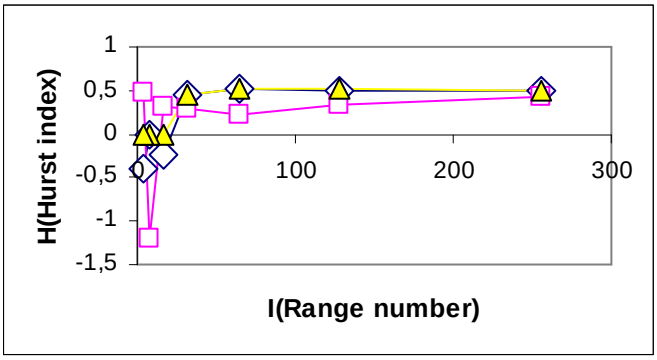

Fig.4. Dependence of H_H for different donors on intensity I range for histograms in Fig.2a; numbers of channels for fluorescence intensity are varied from 4 to 256

Figs. 4 illustrate as much information is lost with the reduction of numbers of measurement channels. Changes are connected with the different qualitative nature of correlations for different scales of averaging. Hurst exponents change persistent (H>1/2) to anti-persistent (H<1/2) behaviors due to range reduction for all cases in Fig.4.

Fig. 4 gives also some illustrations of immunofluorescence networks evolution with the oxidant activity of DNA for different health status. Non-monotonic dependence of Hurst exponents on the number of columns (range) with a decrease in the number of columns (range) to the values I <32 for square points (good health) can not be unambiguously and accurately discussed. In this case, Hurst exponents are individual and depend on many unknown factors (see Fig.6 for healthy man).

3 Fluorescence changeability for healthy donor

Let us examine three examples of changeability of immunofluorescence histograms for a healthy donor. Noticeable variations of initial histograms in Figs. 5a and b give practically identical final quadratic approximations of Shannon entropies in Fig. 5c. Thus it indicates the stability, with insignificant and unessential changes, i.e. good health status of the observed healthy donor during one year.

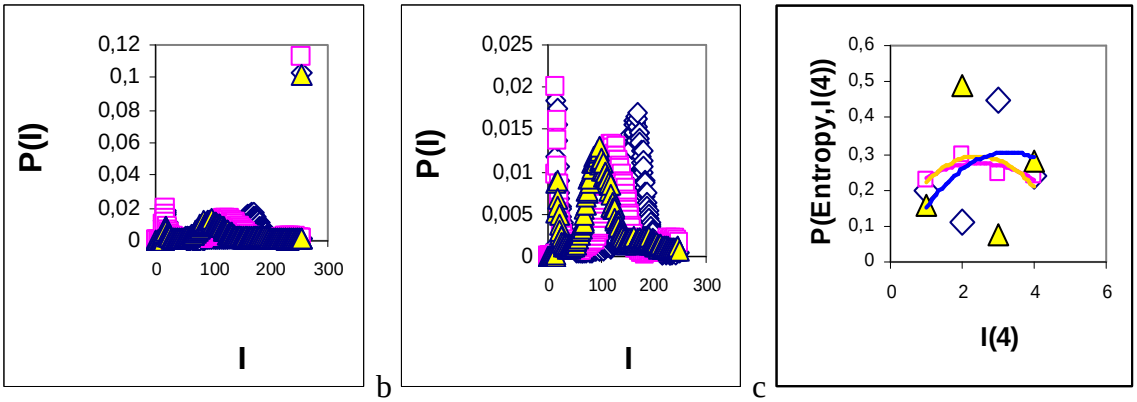

a b c

Fig. 5. Immunofluorescence histograms: initial (a), only central part of histograms (b) and averaged parabolic approximations of ranged Shannon entropy histograms (c) for one, invariably healthy, donor at different times. Rhomb points correspond to the total flashes number $N_0 = 30832$, analysis time is 19 July (first year); triangle points correspond to the total flashes number $N_0 = 38758$, analysis time is 11 July (next year); square points correspond to the total flashes number $N_0 = 40109$,analysis time is 03 June, before 11 July. Local differences between the original histograms for triangle and square points in Figs. 5a

and b are significant. Red and yellow lines of parabolic approximations for triangle and square points in Fig.5c practically coincide. Good health corresponds to rather stable convex parabola approximation for ranged histograms in Fig.5c.

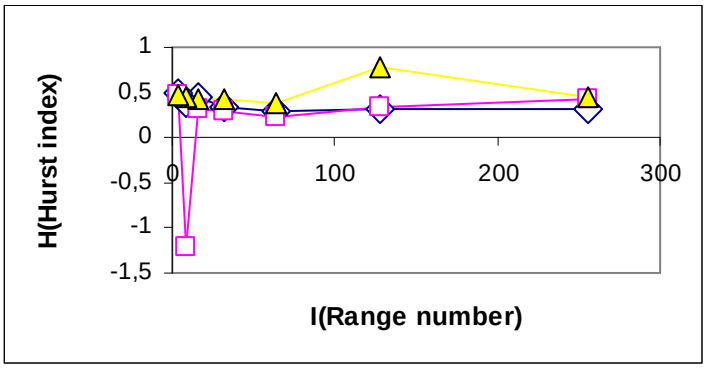

Fig.6. Dependence of H_H for one healthy donor on intensity I range for different histograms in Figs.5; numbers of channels for intensity are varied from 4 to 256

Square points in Figs.1, 2, 3, 4, 5, 6 relate to one healthy donor at one time.

Good health corresponds to rather stable anti-persistent behavior of H<0,5, for range number less than 200. Immunofluorescence networks structure of healthy people is more chaotic than for no good health (see also Fig.4 and companionably small Hurst index for lower line in Fig.3b).

4 Fluorescence changeability for oncology in medical treatment

Let us examine two examples the changeability of immunofluorescence histograms for oncology due to medical treatment (Fig. 7). Detail description of this example contains in [4].

Let us examine an example of oncology sick. In the medical treatment process patient was infected by hepatitis B. Thus we have a complex combination of incurable diseases of inflammatory and autoimmune nature. Sequential treatment of only one disease leads to deterioration in the presence of a second disease. These dramatic metamorphoses have shown in Figs.7.

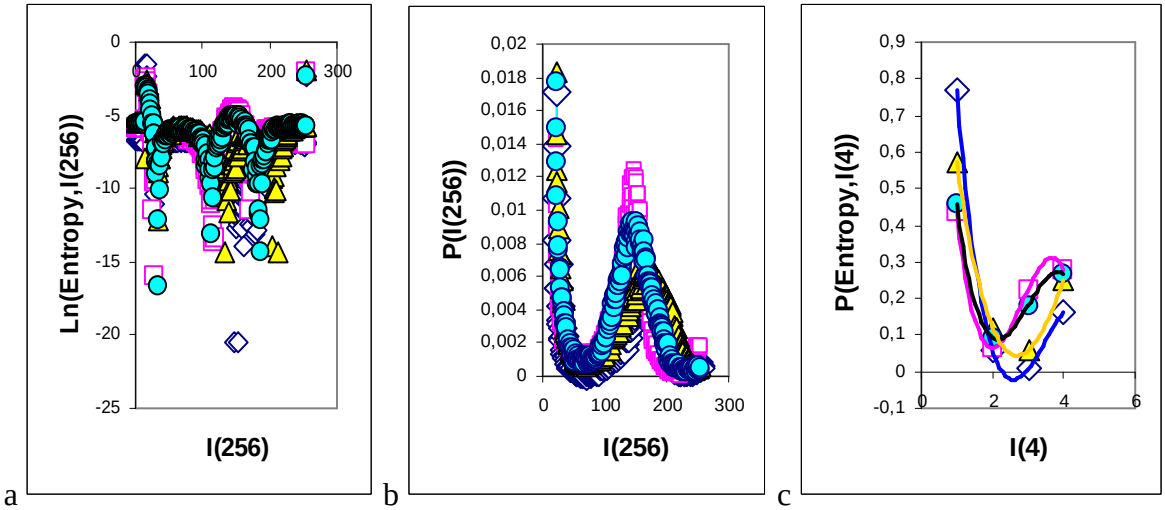

a b c

Fig.7. Dependence of normalized spontaneous fluorescence flashes number P on their intensity I. Symbol rhomb relates to histogram of unhealthy donor; analysis date is 05 November, common number of flashes is N_0=43752. Symbol quadrate corresponds to 15 December, after treatment of hepatitis B; N_0=26265. Triangle points correspond common number of flashes is N_0=45142, analysis time is 21 March next year; Ring points correspond to the total number of flashes N_0=45981, analysis time is 11 July next year, after the

treatment of oncology diseases (a) Logarithm of Shannon entropy distribution (b) for more clearest only central part of initial histograms P(I(256)) (c) averaged cubic parabola approximations of ranged Shannon entropy histograms

At first standard medical treatment against the hepatitis leads to decreasing of inflammation i.e. common number of flashes N_0=43752 down to N_0=26265. Correspondence entropy evolution has shown that concave parabola for rhomb points in Figs.7c transforms to concave-convex parabola for quadrate points in Figs.7c.Concave-convex parabola characterizes inflammatory diseases (see Fig. 2b for asthma). In means that initial oncology dominant exchange on hepatitis dominant, while standard biochemical tests have shown that hepatitis suppressed. Further degradation of the patient health leads to concave parabola for triangle points in Fig. 7c, as for oncology. Next medical treatment associated with activated lymphocytes, improved patient conditions, which describe the concave-convex parabola for ring points in Fig. 7c, as for inflammatory diseases (hepatitis). We observe how the treatment of one of the incurable disease leads to the manifestation of no-good health in the presence of other incurable illness. However, treatment can not be called very unfortunate, because the reduction of networks for immunofluorescence information entropy in Fig, 8 is the same to the reduction of networks for healthy person in Fig. 6. In this case, the medical treatment had extended the life of the patient.

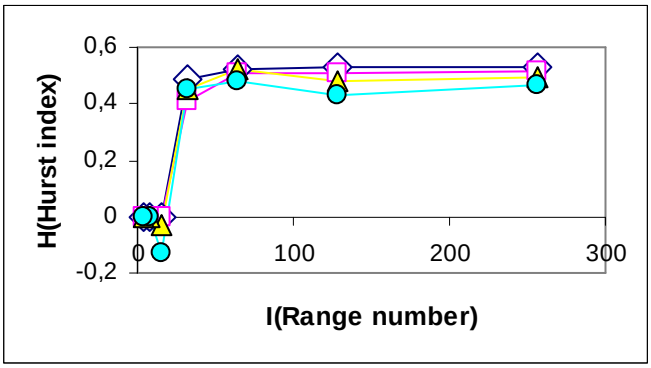

Fig.8. Dependence of H_H for one unhealthy donor on intensity I range for histograms in Figs.7; numbers of channels for averaged fluorescence intensity are varied from 4 to 256

Here oncology disease is complicated by hepatitis B. Oncology disease domains without medical treatment as concave parabolas in Fig.7c. Hepatitis visualized after its standard and substandard medical treatment as concave-convex parabolas in Fig.7c. This example characterizes the reproducible and systematic differences between the health status registrations by immunoflorescence histograms for oncology disease before and after different medical treatment.

5 Results

More simple results are observed for minimal histogram's range in Figs.2b, 5c, 7c. In Figs.2b, 5c, 7c the good-health condition describes by means of convex parabola dominant of parabolic approximation for entropy distribution. In Fig.2b the illness condition describes by means of concave and concave-convex parabola dominant of parabolic approximations for information entropy distributions. Actually, this is one of universal answers on the question about health and illness, which gives the nuclear DNA fluorescence for many thousands-cells of neutrophils population. This is equivalent of estimations of general positive or negative health status as signal of clear reactions from of the immune system.

Hurst exponents can vary monotonically and non-monotonically. Transitions from persistent to anti-persistent Hurst indices are observed due to histogram's range reduction for

all health statuses. These features reflect a complex hierarchy of immunofluorescence networks for different averaging scales and vary for different diseases.

Figs. 4, 6, 8 illustrate as much information is lost with the reduction of numbers of measurement channels. Changes are connected with the different qualitative nature of correlations for different scales of averaging. Very cheap cytometric devices with a small number of measurement channels have pros and cons for the scientific information.

6 Discussion

The stock of health has no price, and the immune system can not be deceived. Different analogies of Hurst index for immunofluorescence bio-nets with Hurst index behavior for foundational and currency markets also may be discussed if we interested in knowledge about good or no-good health of finance, such as stability, inflammation or autoimmunity problems.

7 Conclusions

Preliminary experiments had shown the usage opportunities of proposed approach for the solution of various medical problems. We observed the inflammatory processes after different surgical interventions, post infection complications, neurological and heart complications after diphtheria, chronic inflammation with rheumatoid arthritis, bronchial asthma, course of inflammatory events with the myocardial infarctions, inflammations with system lupus erythematosis, hepatitis, peritonitis, purulent appendicitis, pneumonias, cardiovascular, oncology and other diseases, connected with the oxidants or other reasons for the disturbance of oxidizing metabolism.The spectrum of medical applications, possibly, is considerably wider, because of the wide prevalence of oxidative abnormality as the reason of various illnesses and the aging[5].

To be continued.

References

[1] Robinson J.P., Carter Wane O., Narayanan P. K. Oxidative product formations analysis by flow cytometry. Methods in cell biology, vol.41, Academic press 1994

[2]. Filatov M.V, Varfolomeeva E. Y., Ivanov E.A. Flow cytofluorometric detection of inflammatory processes by measuring respiratory burst reaction of peripheral blood neutrophils. Biochemical and molecular medicine. 1995. Vol. 55, P. 116-121.

[3]. Vladescu I.D., McCauley M.J., Rouzina I., Williams M.C. Mapping the phase diagram of single DNA molecules forced-induced melting in the presence of ethidium. Phys. Rev. Lett**.** 2005. Vol. 95, P. 158102.

[4]. Galich N.E., Filatov M.V. Delay, change and bifurcation of the immunofluorescence distribution attractors in health statuses diagnostics and in medical treatment. Proc. SPIE Vol. 7377, 73770C Jun. 16, 2009

[5]. Galich N.E. Cytometric Distributions and Wavelet Spectra of Immunofluorescence Noise in Medical Diagnostics O. Dossel and W.C. Schlegel (Eds.): WC 2009, IFMBE Proceedings 25/IV, P. 1936–1939, Munich 2009.www.springerlink.com

[6]. Feder J, Fractals, Plenum Press, NewYork, 1988

[7]. Da Silva S., Matsushita R., Gleria I. , Figueiredo A. Hurst exponents, power laws, and efficiency in the Brazilian foreign exchange market. Economics Bulletin, Vol. 7, No. 1 pp. 1-11,2007

[8]. Gagnon J.-S., Lovejoy S., Schertzer D. Multifractal earth topography Nonlin. Processes Geophys., 13, 541–570, 2006

[9]. Lovejoy S., Schertzer D. Scaling and multifractal fields in the solid earth and topography. Nonlin. Processes Geophys., 14, 465–502, 2007